Effect of ballistic electrons on ultrafast thermomechanical responses of a thin metal film*

Qi-lin Xiong(熊启林)[1,2,†] and Xin Tian(田昕)[3]

[1] Department of Mechanics, Huazhong University of Science & Technology, Wuhan 430074, China
[2] Hubei Key Laboratory of Engineering Structural Analysis and Safety Assessment, Wuhan 430074, China
[3] School of Mechanical Engineering, Xi'an Jiaotong University, Xi'an 710049, China

(Received 1 November 2016; revised manuscript received 20 April 2017; published online 18 July 2017)

The ultrafast thermomechanical coupling problem in a thin gold film irradiated by ultrashort laser pulses with different electron ballistic depths is investigated via the ultrafast thermoelasticity model. The solution of the problem is obtained by solving finite element governing equations. The comparison between the results of ultrafast thermomechanical coupling responses with different electron ballistic depths is made to show the ballistic electron effect. It is found that the ballistic electrons have a significant influence on the ultrafast thermomechanical coupling behaviors of the gold thin film and the best laser micromachining results can be achieved by choosing the specific laser technology (large or small ballistic range). In addition, the influence of simplification of the ultrashort laser pulse source on the results is studied, and it is found that the simplification has a great influence on the thermomechanical responses, which implies that care should be taken when the simplified form of the laser source term is applied as the Gaussian heat source.

Keywords: ultrafast thermomechanical coupling, ballistic electrons, ultrashort laser pulse, finite element method

PACS: 65.40.De, 62.25.–g **DOI:** 10.1088/1674-1056/26/9/096501

1. Introduction

The investigation of interactions between femtosecond lasers and thin metal films is drawing increasing attention.[1,2] For femtosecond pulses, it has been assumed that the laser energy is primarily absorbed by the free electrons that are confined close to the surface. Hence, a strong nonequilibrium between the energy carriers, namely, the electrons and phonons, is created in this process. In this highly nonequilibrium state, ballistic motion of electrons into deeper parts of the sample with velocities close to the Fermi velocity will take place. The ballistic energy transport occurring before the thermalization of the electron gas has been found to play an important role in the initial energy redistribution in targets irradiated by femtosecond laser pulses.[3–6]

Due to the complexity of the process of ballistic electrons transport, most investigations cannot offer the non-equilibrium electron distributions in the sample exactly. It is a good choice to add the ballistic range to the laser penetration depth in the laser source term to incorporate this effect of ballistic electrons,[4,7–10] as given below:

$$Q(x,t) = \frac{(1-R)\sqrt{\beta/\pi}J_0}{(x_s+\lambda_{ball})\left[1-\exp\left(-L/x_s+\lambda_{ball}\right)\right]} \times \exp\left[-\left(\frac{x}{x_s+\lambda_{ball}}\right)\right], \quad (1)$$

where x_s is the transmission depth of the laser, J_0 is the laser fluence, R is the reflection coefficient of the laser pulse, t_p is the laser pulse duration and constant, and β is equal to 4ln(2). Here λ_{ball} is the ballistic range. However, the ballistic range has taken different values from tens of nanometers to hundreds of nanometers for the same material in different works. In some works, equation (1) is simplified as follows:

$$Q(x,t) = \frac{(1-R)\sqrt{\beta/\pi}J_0}{x_s}\exp\left[-\left(\frac{x}{x_s+\lambda_{ball}}\right)\right]. \quad (2)$$

In fact, the ballistic range can take different values for different laser types, such as CO_2 lasers (gas lasers), fiber lasers, Nd:YAG (crystal lasers). According to the work of Thomsen *et al.*,[11] the laser penetration depth $(x_s+\lambda_{ball})$ can be estimated by

$$x_s+\lambda_{ball} = \frac{\lambda}{4\pi\kappa}, \quad (3)$$

where λ is the wavelength of the laser and κ is the imaginary part of the refraction index of the thin film. Due to the significant difference of laser wavelength between different laser types,[12] the laser penetration depth can be varied from a few nanometers to several hundred nanometers.

The main aim of this work is to investigate the effect of ballistic electrons on ultrafast thermomechanical coupling behaviors and the influence of simplification of the laser source term. The numerical results can provide a theoretical guid-

*Project supported by the National Natural Science Foundation of China (Grant No. 11502085), the Natural Science Foundation of Hubei Province, China (Grant No. 2016CFB542), the Fundamental Research Funds for the Central Universities, China (Grant No. 2016YXMS097), and the Research Fund of State Key Laboratory of Mechanics and Control of Mechanical Structures (NUAA), China (Grant No. 0315K01).

†Corresponding author. E-mail: xiongql@hust.edu.cn

© 2017 Chinese Physical Society and IOP Publishing Ltd

ance for choice and application of the laser type against different engineering requests. The ultrafast thermoelasticity (UTE) model developed by Chen *et al.*[13] extending the dual-hyperbolic two-temperature and hot-electron blast model[14] is applied to study the ultrafast thermomechanical behaviors of a gold film subjected to femtosecond laser heating in the present work. The finite element method is applied to solve the problem in the present work due to the successful usage of finite element method in the investigations of thermomechanical responses of metallic films under ultrashort pulse laser heating.[15,16]

2. Mathematical model

An immense homogeneous, isotropic, gold thin film ($0 \leq x \leq L$, L is the film thickness, $L = 2$ μm) whose surface is heated by laser beams of radius r_0 is considered in this work ($r_0 >> L$). In view of the fact that ultrafast deformation takes place in a very short period of time, it is assumed that both the thermal transport and the lattice deformation do not occur immediately in directions normal to the thickness direction. Therefore, within the heated spot the thermal transport can be treated as a 1D process and the mechanical response is in a state of uni-axial strain but 3D stress.[15,16]

The field equations of the ultrafast thermoelasticity (UTE) model developed by Chen *et al.*[13] extending the dual-hyperbolic two-step heat transfer and hot-electron blast models[14] are given as follows:
heat conduction equations

$$\tau_{\mathrm{e}}(T_{\mathrm{e}})\dot{q}_{\mathrm{e}} + q_{\mathrm{e}} = -K_{\mathrm{e}}(T_{\mathrm{e}}, T_{\mathrm{l}})\nabla T_{\mathrm{e}}, \tag{4}$$

$$\tau_{\mathrm{l}}\dot{q}_{\mathrm{l}} + q_{\mathrm{l}} = -K_{\mathrm{l}}\nabla T_{\mathrm{l}}, \tag{5}$$

$$C_{\mathrm{e}}(T_{\mathrm{e}})\dot{T}_{\mathrm{e}} = -\nabla q_{\mathrm{e}} - G(T_{\mathrm{e}} - T_{\mathrm{l}}) + Q, \tag{6}$$

$$C_{\mathrm{l}}\dot{T}_{\mathrm{l}} = -\nabla q_{\mathrm{l}} + G(T_{\mathrm{e}} - T_{\mathrm{l}}) - (3\lambda + 2\mu)\alpha T_{\mathrm{l}}\dot{e}_{kk}, \tag{7}$$

constitutive equation

$$\sigma_{ij} = \lambda e\delta_{ij} + 2\mu\varepsilon_{ij} - \gamma(T_{\mathrm{l}} - T_0)\delta_{ij}, \tag{8}$$

equations of motion

$$\sigma_{ji,j} + \Lambda(T_{\mathrm{e}})^2_{,i} = \rho\ddot{u}_i, \tag{9}$$

strain–displacement relations

$$\varepsilon_{ij} = \frac{1}{2}(u_{i,j} + u_{j,i}). \tag{10}$$

In the above equations, $\tau_{\mathrm{e}} = 1/(A_{\mathrm{e}}T_{\mathrm{e}}^2 + B_{\mathrm{l}}T_{\mathrm{l}})$, $C_{\mathrm{e}}(T_{\mathrm{e}}) = C_{\mathrm{e}0}T_{\mathrm{e}}/T_0$, $C_{\mathrm{e}0}$ is the electron specific heat at T_0. $K_{\mathrm{e}}(T_{\mathrm{e}}, T_{\mathrm{l}}) = K_{\mathrm{e}0}T_{\mathrm{e}}/T_{\mathrm{l}}$, $K_{\mathrm{e}0}$ is the electron thermal conductivity at T_0. ∇ is the gradient operator. In the equations, a comma followed by a suffix denotes the material derivative and the superposed dot denotes the derivative with respect to time.

For a solid medium irradiated by a Gaussian laser beam, the volumetric laser heat source $Q(x,t)$ without ballistic range in Eq. (10) is expressed in the 1D form

$$Q(x,t) = \sqrt{\frac{\beta}{\pi}}J_0\frac{1-R}{t_{\mathrm{p}}x_{\mathrm{s}}}\exp\left[-\left(\frac{x}{x_{\mathrm{s}}}\right) - \beta\left(\frac{t}{t_{\mathrm{p}}} - 2\right)^2\right]. \tag{11}$$

The laser power outside the period of the lasing time assumed here is ignored because of the small amount of energy.

When the effect of the ballistic electrons is considered, the Gaussian laser source term can be changed to[4,7–10]

$$Q(x,t) = \sqrt{\frac{\beta}{\pi}}J_0\frac{(1-R)}{t_{\mathrm{p}}(x_{\mathrm{s}} + \lambda_{\mathrm{ball}})[1 - \exp(-L/x_{\mathrm{s}} + \lambda_{\mathrm{ball}})]} \times \exp\left[-\left(\frac{x}{x_{\mathrm{s}} + \lambda_{\mathrm{ball}}}\right) - \beta\left(\frac{t}{t_{\mathrm{p}}} - 2\right)^2\right]. \tag{12}$$

The simplified form of the Gaussian laser source term with the effect of the ballistic electrons is as follows:[17]

$$Q(x,t) = \sqrt{\frac{\beta}{\pi}}J_0\frac{(1-R)}{x_{\mathrm{s}}t_{\mathrm{p}}} \times \exp\left[-\left(\frac{x}{x_{\mathrm{s}} + \lambda_{\mathrm{ball}}}\right) - \beta\left(\frac{t}{t_{\mathrm{p}}} - 2\right)^2\right]. \tag{13}$$

Under the uniaxial strain condition

$$\varepsilon_{xx} \neq 0, \varepsilon_{yy} = \varepsilon_{zz} = \varepsilon_{xy} = \varepsilon_{xz} = \varepsilon_{yz} = 0, \tag{14}$$

the three normal stress components become

$$\sigma_{xx} = (\lambda + 2\mu)u_{x,x} - \gamma(T_{\mathrm{l}} - T_0), \tag{15}$$

$$\sigma_{yy} = \sigma_{zz} = \lambda u_{x,x} - \gamma(T_{\mathrm{l}} - T_0). \tag{16}$$

From the preceding description and the problem we will consider, the initial and boundary conditions may be expressed as follows:
initial conditions ($t = 0$):

$$u_x(x,0) = \dot{u}_x(x,0) = 0,$$
$$T_{\mathrm{e}}(x,0) = T_{\mathrm{l}}(x,0) = T_0,$$
$$\sigma_{xx}(x,0) = 0;$$

boundary conditions ($x = 0$):

$$q_{\mathrm{e}}(0,t) = q_{\mathrm{e}}(L,t) = 0,$$
$$q_{\mathrm{l}}(0,t) = q_{\mathrm{l}}(L,t) = 0,$$
$$\sigma_{xx}(0,t) = \sigma_{xx}(0,L) = 0.$$

3. Solutions of the finite element equations of problem

According to the heat conduction equations, equations of motion, constitutive equations, and boundary conditions, using the generalized variational principle, we obtain at any time

$$\int_v \left[\delta\{\varepsilon\}^{\mathrm{T}}\left(\{\sigma\} + 2\Lambda\{T_{\mathrm{e}}\}^{\mathrm{T}}\{T_{\mathrm{e}}\}\right) + \delta\left\{T'_{\mathrm{e}}\right\}^{\mathrm{T}}\{q_{\mathrm{e}} + \tau_{\mathrm{e}}\dot{q}_{\mathrm{e}}\} + \delta\left\{T'_{\mathrm{l}}\right\}^{\mathrm{T}}\{q_{\mathrm{l}} + \tau_{\mathrm{l}}\dot{q}_{\mathrm{l}}\}\right.$$

$$
\begin{aligned}
&+ \delta T_{\mathrm{e}}(\nabla \cdot \boldsymbol{q}_{\mathrm{e}} + \tau_{\mathrm{e}} \nabla \cdot \dot{\boldsymbol{q}}_{\mathrm{e}} - Q - \tau_{\mathrm{e}} \dot{Q}) \\
&+ \delta T_{\mathrm{l}}(\nabla \cdot \boldsymbol{q}_{\mathrm{l}} + \tau_{\mathrm{l}} \nabla \cdot \dot{\boldsymbol{q}}_{\mathrm{l}})\Big] \mathrm{d}V \\
&= \int_v \delta \{u\}^{\mathrm{T}} (-\rho \{\ddot{u}\}) \mathrm{d}V + \int_{A_\sigma} \delta \{u\}^{\mathrm{T}} \{T'\} \mathrm{d}A \\
&+ \int_{A_{q_{\mathrm{e}}}} \delta T_{\mathrm{e}} \bar{q}_{\mathrm{e}} \mathrm{d}A + \int_{A_{q_{\mathrm{l}}}} \delta T_{\mathrm{l}} \bar{q}_{\mathrm{l}} \mathrm{d}A. \qquad (17)
\end{aligned}
$$

At the right side of the above equation, T', $\bar{q}_{\mathrm{e}}$, and $\bar{q}_{\mathrm{l}}$ are the external force vector, the external electron heat flux, and the external lattice flux vector, respectively. Then the finite element governing equations can be established and solved in the time domain directly by associating with the corresponding initial conditions and boundary conditions.

4. Results and discussion

Due to the ultrashort interaction time, the thermal loss at the surface of the gold film is ignored in all the calculations. The temperature-dependent thermal conductivity and heat capacity of the gold electron are given in the previous section. All thermophysical properties of gold used in the modeling are as follows:

$$
\begin{aligned}
&\rho = 19300\ \mathrm{kg \cdot m^{-3}},\ C_{\mathrm{e0}} = 2.1 \times 10^4\ \mathrm{J \cdot m^{-3} \cdot K^{-1}}, \\
&G = 2.6 \times 10^{16}\ \mathrm{W \cdot m^{-3} \cdot K^{-1}},\ \Lambda = 70 \mathrm{J \cdot m^{-3} \cdot K^{-2}}, \\
&\alpha_t = 14.2 \times 10^{-6}\ \mathrm{K^{-1}},\ k_{\mathrm{e0}} = k_{\mathrm{l}} = 315\ \mathrm{W \cdot m^{-1} \cdot K^{-1}}, \\
&A_{\mathrm{e}} = 1.2 \times 10^7\ \mathrm{K^{-2} \cdot s^{-1}},\ B_{\mathrm{l}} = 1.23 \times 10^{11}\ \mathrm{K^{-1} \cdot s^{-1}}, \\
&E = 74.9\ \mathrm{GPa},\ \nu = 0.42,\ \tau_{\mathrm{l}} = 38.7\ \mathrm{ps},\ R = 0.93, \\
&x_{\mathrm{s}} = 15.3\ \mathrm{nm},\ J_0 = 2000\ \mathrm{J/m^2}.
\end{aligned}
$$

First of all, we make the validation of the finite element method applied in the present study and the problem in Ref. [10] is reinvestigated. Figures 1 and 2 compare the numerically predicted electron and lattice temperatures with those of Ref. [10]. It is found that the electron and lattice temperatures predicted by the finite element method agree very well with those in the reference.

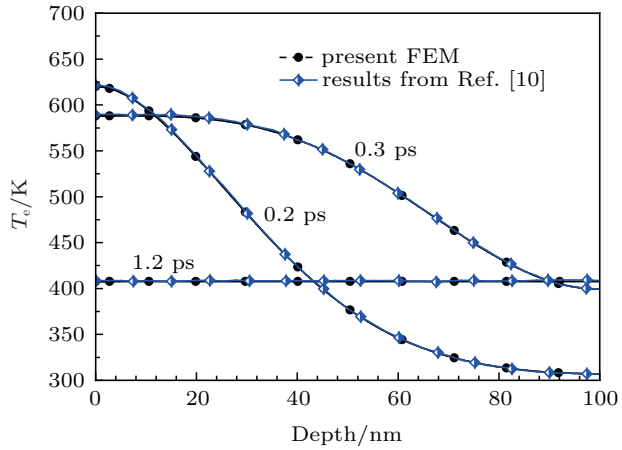


Fig. 1. (color online) Electron temperature profiles for a 100-nm gold film heated by a 100-fs laser pulse of $J_0 = 10$ J/m^2.

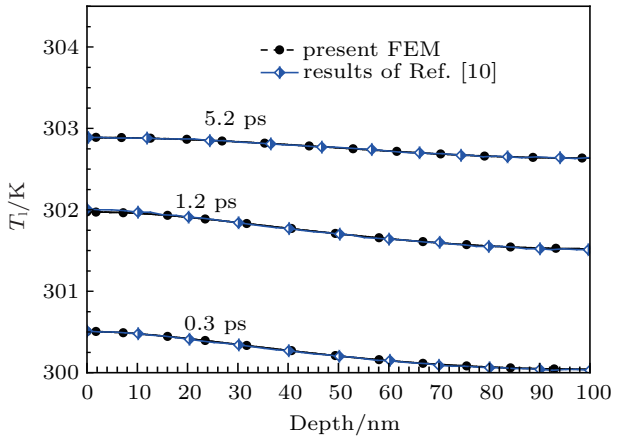


Fig. 2. (color online) Lattice temperature profiles for a 100-nm gold film heated by a 100-fs laser pulse of $J_0 = 10$ J/m^2.

4.1. The effect of ballistic electron on the thermomechanical response

Figure 3 shows the electron temperature at the top surface under different ballistic ranges: (a) without ballistic effect; (b) $\lambda_{\mathrm{ball}} = 105$ nm; (c) $\lambda_{\mathrm{ball}} = 500$ nm. The highest electron temperatures of the three cases are 8.51×10^3 K, 4.94×10^3 K, and 2.67×10^3 K, respectively. The highest electron temperature decreases with the increase of the ballistic range, this is due to the fact that the optical penetration depth of the laser pulse is large and the laser energy is dispersed spatially; the total optical penetration depths of the three laser pulses are 15.3 nm, 120.3 nm, and 515.3 nm, respectively.

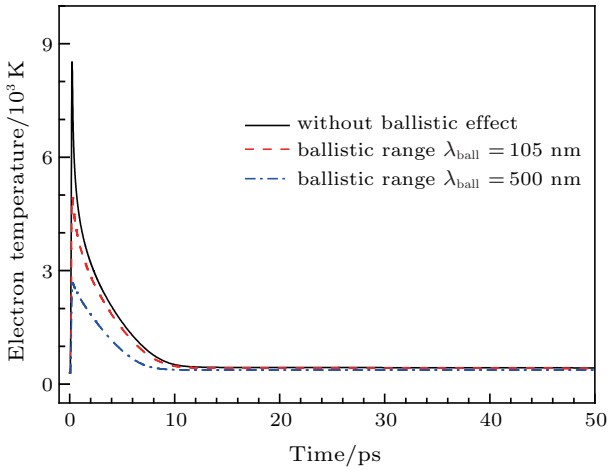


Fig. 3. (color online) Electron temperature at the top surface versus time under different ballistic ranges. The top surface is the surface irradiated by the laser pulse.

Figure 4 shows the spatial distributions of electron temperature with different ballistic ranges at several time points. With the increase of the ballistic range, the electron temperature near the top surface decreases whereas the electron temperature of deep region in the film increases. When the ballistic range increases, the laser energy can be transferred to the deeper region of the film. Since the total laser energy is constant, the electron temperature in the thin film is affected by the ballistic range; the larger the ballistic range, the lower

the electron temperature near the top surface, and the higher the electron temperature in the deep region of the thin film, as shown in Fig. 4. These results show the effect of the ballistic electron has a great influence on the electron temperature.

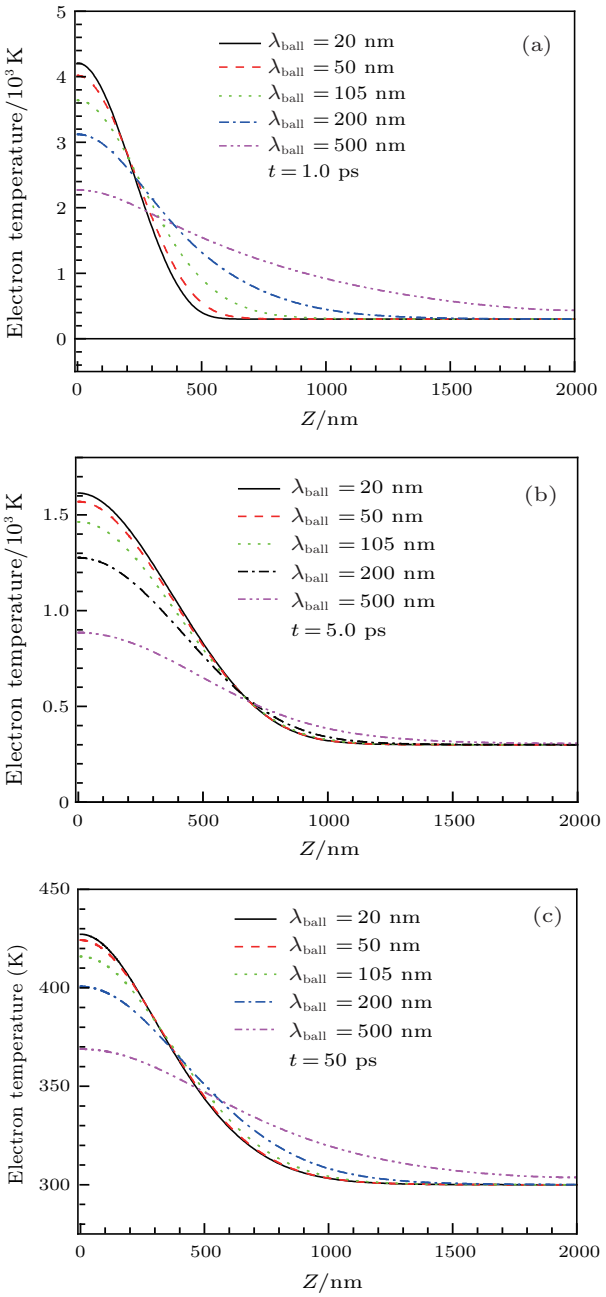


Fig. 4. (color online) The spatial distributions of electron temperature with different ballistic ranges at several time points: (a) 1.0 ps, (b) 5 ps, (c) 50 ps.

The spatial distributions of the phonon temperature with different ballistic ranges at several time points are shown in Fig. 5. Similarly, with the increase of the ballistic range, the phonon temperature near the top surface decreases, whereas the phonon temperature of deep region in the film increases. Additionally, the highest phonon temperature in the thin film decreases when the ballistic range increases. These results further show that the electron ballistic effect can influence the utilization of the laser pulse technology. Based on these results, we can choose the specific laser technology (long or short wave) to meet the special engineering requirements.

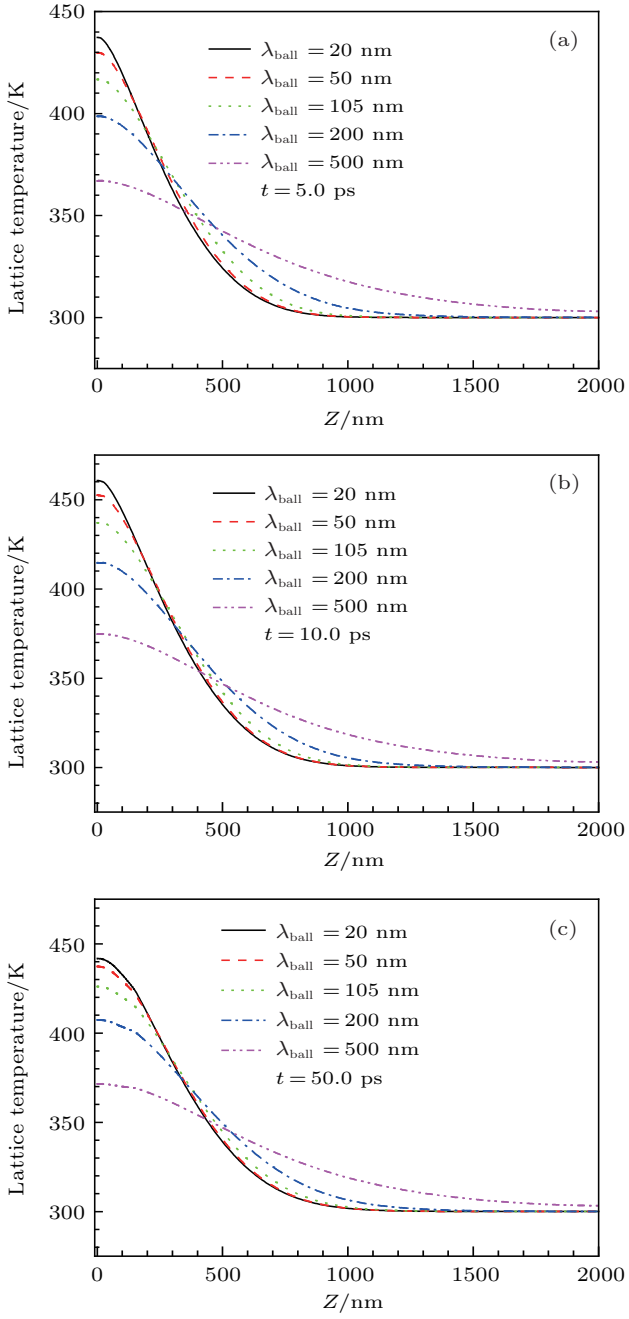


Fig. 5. (color online) The spatial distributions of phonon temperature with different ballistic ranges at several time points: (a) 5.0 ps, (b) 10 ps, (c) 50 ps.

Figure 6 illustrates the spatial distributions of the hot-electron blast force $(2\Lambda T_e(\partial T_e/\partial z))$[10,11] with different ballistic ranges at several time points. From Fig. 6, it is seen that the hot-electron blast force in the thin film decreases dramatically with the increase of the ballistic range and the hot-electron blast force is confined in the small region near the top surface, which indicates that the electron ballistic effect has a significant influence on the hot-electron blast force.

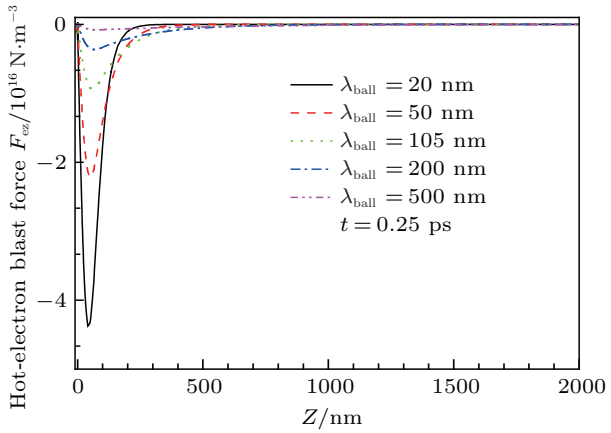


Fig. 6. (color online) The spatial distributions of hot-electron blast force $(2\Lambda T_e(\partial T_e/\partial z))$ with different ballistic ranges at $t = 0.25$ ps.

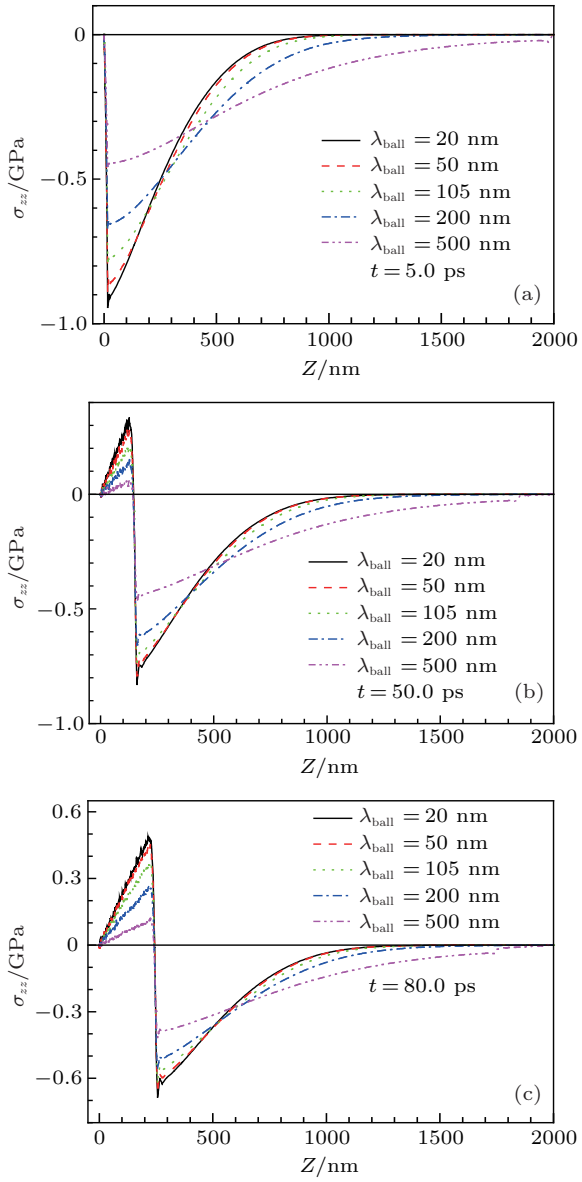


Fig. 7. (color online) The spatial distributions of stress with different ballistic ranges at several time points: (a) 5.0 ps, (b) 50 ps, (c) 80 ps.

The spatial distributions of stress with different ballistic ranges at several time points are shown in Fig. 7. With the increase of the ballistic range, the highest absolute value of stress in the thin film decreases whereas the region disturbed in the film increases. This is due to the fact that the laser energy diffuses into the deep region of the film when the ballistic range increases. These results show that the electron ballistic effect can influence the stress distribution of the thin film. It can be deduced that according to different engineering requirements, different laser types can be utilized to achieve the best machining results.

Figure 8 shows the spatial distributions of displacement with different ballistic ranges at several time points. Similarly, with the increase of the ballistic range, the highest absolute value of displacement in the thin film decreases whereas the region disturbed in the film increases. These results further show that the electron ballistic effect can influence the thermomechanical behaviors in the thin film. It further demonstrates that the best machining results can be achieved by choosing the specific laser technology.

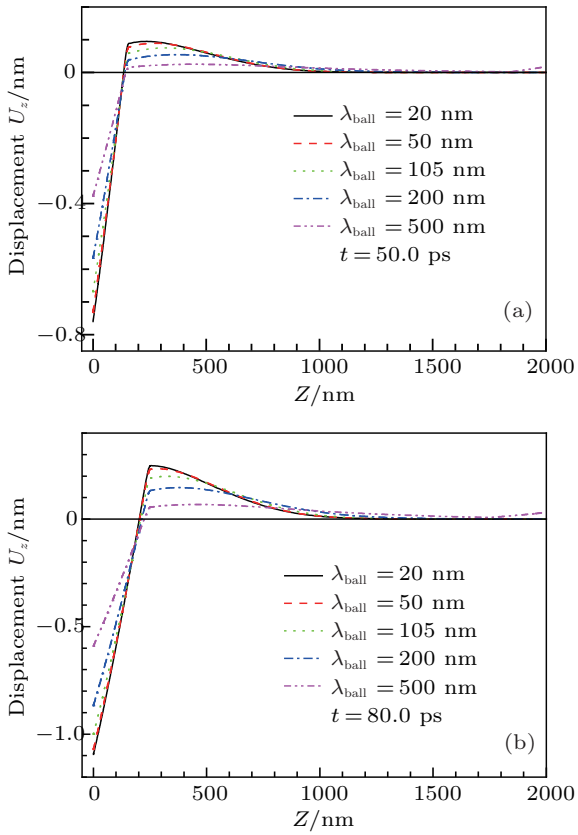


Fig. 8. (color online) The spatial distributions of displacement with different ballistic ranges at several time points: (a) 50 ps, (b) 80 ps.

4.2. The influence of simplification of laser source term on the thermomechanical response

The spatial distributions of electron temperature, phonon temperature, stress, and displacement in the gold thin film under two conditions of ballistic range $\lambda_{ball} = 105$ nm and simplified form $\lambda_{ball} = 105$ nm at several time points are shown in Figs. 9–12, respectively. The simplification of the laser source

term makes the thermomechanical responses increase significantly, which shows that the simplification of the laser source term has a great influence on the thermomechanical responses of the thin film. This implies that care should be taken when the simplified form of the laser source term is applied as the Gaussian heat source.

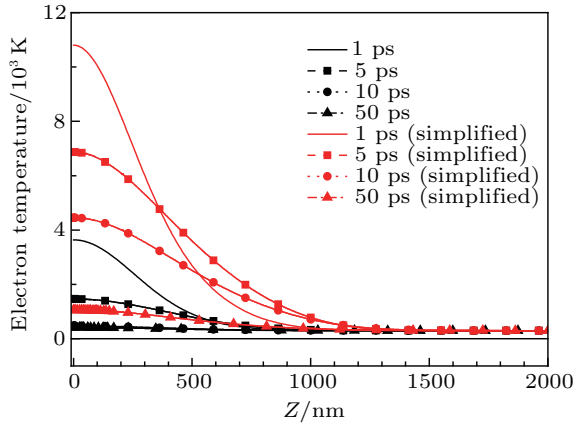


Fig. 9. (color online) The spatial distributions of electron temperature under two conditions of ballistic range $\lambda_{\text{ball}} = 105$ nm and simplified form $\lambda_{\text{ball}} = 105$ nm at several time points.

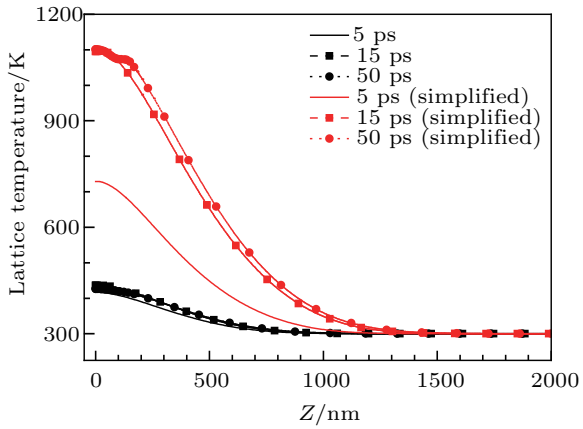


Fig. 10. (color online) The spatial distributions of lattice temperature under two conditions of ballistic range $\lambda_{\text{ball}} = 105$ nm and simplified form $\lambda_{\text{ball}} = 105$ nm at several time points.

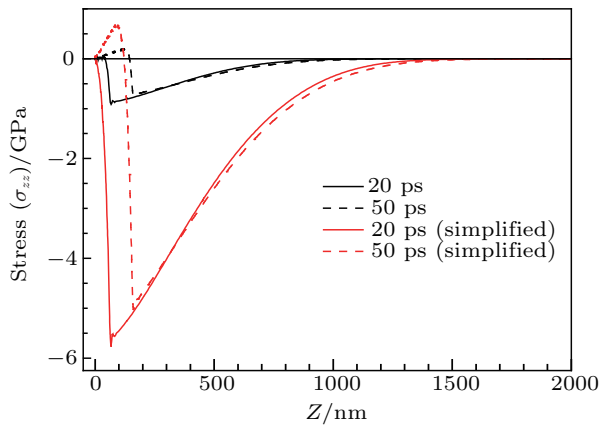


Fig. 11. (color online) The spatial distributions of stress under two conditions of ballistic range $\lambda_{\text{ball}} = 105$ nm and simplified form $\lambda_{\text{ball}} = 105$ nm at several time points.

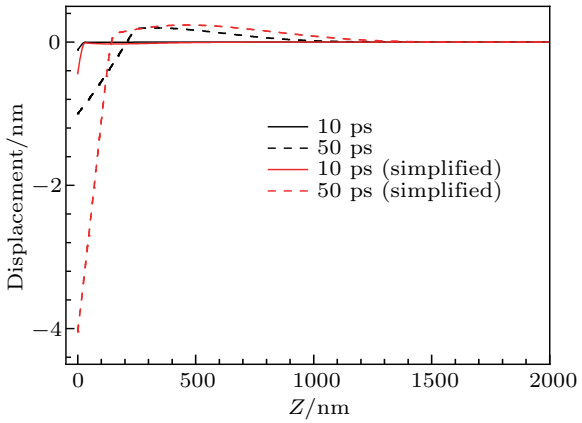


Fig. 12. (color online) The spatial distributions of displacement under two conditions of ballistic range $\lambda_{\text{ball}} = 105$ nm and simplified form $\lambda_{\text{ball}} = 105$ nm at several time points.

5. Conclusion

The effect of ballistic electrons and the influence of simplification of the laser source term on ultrafast thermomechanical coupling behaviors are studied by using the finite element method to investigate the ultrafast thermomechanical coupling response of a gold film impacted by different laser pulses. The results of this study show that the effect of ballistic electrons has a significant influence on the ultrafast thermomechanical coupling behaviors of the gold thin film and the simplification has a great influence on the thermomechanical responses. We conclude that with the increase of the ballistic range, the thermomechanical coupling response near the top surface decreases whereas the region disturbed in the film increases as well as the thermomechanical coupling response of the deep region in the film increases. Additionally, the simplification of the laser source term has a great influence on the thermomechanical responses of the thin film and care should be taken when the simplified form of the laser source term is applied.

References

[1] Liu X, Du D and Mourou G 1997 *IEEE. J. Quantum. Elect.* **33** 1706
[2] Shirk M D and Molian P A 1998 *J. Laser. Appl.* **10** 18
[3] Fujimoto J G, Liu J M and Ippen E P 1984 *Phys. Rev. Lett.* **53** 1837
[4] Hohlfeld J, Wellershoff S S, Gudde J, Conrad U, Jahnke V and Matthias E 2000 *Chem. Phys.* **251** 237
[5] Sua' rez C, Bron W E and Juhasz T 1995 *Phys. Rev. Lett.* **75** 4536
[6] Liu X, Stock R and Rudolph W 2005 *Phys. Rev. B* **72** 195431
[7] Byskov-Nielsen J, Juha-Matti S, Christensen M S and Balling P 2011 *Appl. Phys. A* **103** 447
[8] Thomas D A, Lin Z, Zhigilei L V, Gurevich E L, Kittel S and Hergenröder R 2009 *Appl. Surf. Sci.* **255** 9605
[9] Wellershoff S S, Hohlfeld J, Güdde J and Matthias E 1999 *Appl. Phys. A* **69** 99
[10] Chen J K and Beraun J E 2001 *Numer. Heat. Tr. A-Appl.* **40** 1
[11] Thomsen C, Grahn, H T, Maris H J and Tauc J 1986 *Phys. Rev. B* **34** 4129
[12] Oulton R F, Sorger V J, Zentgraf T, Ma R M, Gladden C, Dai L, Bartal G and Zhang X 2009 *Nature* **461** 629
[13] Chen J K, Beraun J E, Grimes L E and Tzou D Y 2002 *Int. J. Solids. Struct.* **39** 3199
[14] Falkovsky L A and Mishchenko E G 1999 *Sov. Phys. JEPT* **88** 84
[15] Xiong Q L and Tian X G 2013 *J. Therm. Stresses.* **36** 387
[16] Xiong Q L and Tian X G 2015 *Mech. Adv. Mater. Struc.* **22** 548
[17] Gan Y, Qi W J, Shen Y G and Chen Z 2013 *Opt. Lett.* **38** 2397